THE ASTROPHYSICAL JOURNAL, 512:793–803, 1999 February 20

PROBING THE STRUCTURE OF ACCRETING COMPACT SOURCES THROUGH X-RAY TIME LAGS AND SPECTRA

XIN-MIN HUA[1] AND DEMOSTHENES KAZANAS
LHEA, NASA/GSFC Code 661, Greenbelt, MD 20771

AND

WEI CUI
Center for Space Research, MIT, Cambridge, MA 02139
Received 1998 June 26; accepted 1998 September 25

ABSTRACT

We exhibit, by compiling all data sets we can acquire, that the Fourier-frequency–dependent, hard X-ray lags, first observed in the analysis of aperiodic variability of the light curves of the black hole candidate Cyg X-1, appear to be a property shared by several other accreting black hole candidate sources and also by the different spectral states of this source. We then present both analytic and numerical models of these time lags resulting by the process of Comptonization in a variety of hot electron configurations. We argue that, under the assumption that the observed spectra are due to Comptonization, the dependence of the lags on the Fourier period provides a means for mapping the spatial density profile of the hot electron plasma, while the period at which the lags eventually level off provides an estimate of the size of the scattering cloud. We further examine the influence of the location and spatial extent of the soft photon source on the form of the resulting lags for a variety of configurations; we conclude that the study of the X-ray hard lags can provide clues about these parameters of the Comptonization process, too. Fits of the existing data with our models indicate that the size of the Comptonizing clouds are quite large in extent ($\sim$1 lt-s) with inferred radial density profiles that are in many instances inconsistent with those of the standard dynamical models, whereas the extent of the source of soft photons appears to be much smaller than those of the hot electrons by roughly 2 orders of magnitude and its location consistent with the center of the hot electron corona.

Subject headings: accretion, accretion disks — black hole physics — radiation mechanisms: nonthermal — stars: neutron — X-rays: stars

1. INTRODUCTION

The study of the physics of accretion onto compact objects (neutron stars and black holes), whether in Galactic (X-ray binaries) or extragalactic systems (active galactic nuclei [AGNs]), involves length scales much too small to be resolved by current technology or that of the foreseeable future. As such, this study is conducted mainly through the theoretical interpretation of spectral and temporal observations of these systems, much in the way that the study of spectroscopic binaries has been used to deduce the properties of the binary system members and the elements of their orbits. In this endeavor, the first line of attack in uncovering the physical properties of these systems is the analysis of their spectra. Thus there exists a large body of spectral observations, accumulated over the past several decades, indicating that the spectra of this class of objects and, in particular, the black hole candidate (BHC) sources, can be fitted very well by those resulting from the Comptonization of soft photons by hot ($T_e \sim 10^9$ K) electrons; the latter are "naturally" expected to be present in these sources, a result of the dissipation of the accretion kinetic energy within an accretion disk. It is thus generally agreed that Comptonization is the process responsible for the production of the high-energy ($\gtrsim$2–100 keV) radiation in these sources. For this reason, this process has been studied extensively both analytically and numerically over the past couple of decades (see, e.g., Sunyaev & Titarchuk 1980; Titarchuk 1994; Hua & Titarchuk 1995). Thus, while the issue of the detailed dynamics of accretion onto the compact object is still not resolved, there has been ample spectral evidence corroborating the presence of a population of hot electrons, located presumably (for energetic reasons) in its vicinity. Spectral modeling and fits to observations have subsequently been employed as a means of constraining or even determining the dynamics of accretion flows onto the compact object.

It is well known, however, that the Comptonization spectra cannot provide, in and of themselves, any information about the size of the scattering plasma, because they depend (for optically thin plasmas) only on the product of the electron temperature and the plasma Thomson depth. Therefore, they cannot provide any clues about the dynamics of accretion of the hot gas onto the compact object, which require the knowledge of the density and velocity as a function of radius. To determine the dynamics of accretion, one needs, in addition to the spectra, time variability information. It is thought, however, that such information may not be terribly relevant, because it is generally accepted that the X-ray emission originates at the smallest radii of the accreting flow and, as such, time variability would simply reflect the dynamical or scattering timescales of the emission region, of order of milliseconds for Galactic accreting sources and 10^5–10^7 times longer for AGNs. (One should bear in mind, however, that for black holes masses as large as expected in AGNs, the emission associated with the region closest to the black hole may in fact be that of the UV rather than X-ray part of the spectrum, without that invalidating the arguments concerning their X-ray emission, which is also generally accepted to be due to Comptonization.)

[1] Universities Space Research Association.

Variability studies, however, have provided inconclusive results at best; the simplest and most frequently used variability measure, the power spectral density (hereafter PSD), has the following generic, counterintuitive form:

$$|F(\nu)|^2 \propto \nu^{-s} \quad \text{with} \begin{cases} s \simeq 0 & \text{for } \nu < \nu_c \,, \\ s \gtrsim 1 & \text{for } \nu_b > \nu > \nu_c \,, \\ s \simeq 2 & \text{for } \nu > \nu_b \end{cases} \qquad (1)$$

(see, e.g., Miyamoto et al. 1991; Belloni et al. 1996; Grove et al. 1997; Cui et al. 1997b), where $\nu_c \simeq 0.3$ Hz and $\nu_b \gtrsim$ 3–10 Hz. The surprising feature of PSDs with the above form is that most of the variability power resides around $\nu \simeq \nu_c$, a frequency 3–4 orders of magnitude lower than the kHz range characteristic of the presumed dynamics of infall onto the compact object. There is a fair amount of variability power between ν_c and $\nu_b \simeq 10$ Hz, with the PSD slope being flatter than the value corresponding to simple exponential shots ($s = 2$) and consistent with the slope of "flicker noise" ($s \simeq 1$), a fact thought to be of significance for understanding the underlying dynamics. However, it is our opinion that of greater significance is the marked absence of variability at the anticipated kHz range of frequencies, in view of the fact that the apparently thin emission requires infall velocities close to that of free–fall. This latter fact implies, then, that the flows near the compact object should have a significant turbulent component associated with the viscosity necessary to yield the inferred large infall velocities; we find of interest that the presence of this turbulence is not apparent in the observed X-ray variability, as measured by the PSD. It is worth noting that a similar lack of variability at the expected frequencies was also found for AGNs by Tennant & Mushotzky (1983) in the HEAO-1 database. The PSDs of AGN X-ray light curves, although not as firmly established as those of Galactic BHCs, appear nonetheless to indicate a similar lack of variability at the corresponding anticipated frequency range ($\sim 10^{-2.5}$ Hz), with most of the power at significantly lower frequencies ($\sim 10^{-6}$ Hz; Green et al. 1993).

This discrepancy between the expected and observed variability is generally attributed to a modulation of the accretion rate onto the compact object, thus deferring an account of the PSD form to a more thorough understanding of the dynamics of accretion. However, the Comptonization process, thought to be responsible for the high-energy emission, offers an alternative measure of variability more refined than the PSD (see, e.g., van der Klis et al. 1987; Wijers, van Paradijs, & Lewin 1987): in this process, the energy of the scattered soft photons increases on the average with their residence time in the scattering medium; as a result, the hard photon light curves lag with respect to those of softer photons by amounts that are roughly proportional to the photon scattering time and the logarithm of the photon energy ratio. Thus observations of these time lags provide a measure of the local electron density or, in an optically thin medium ($\tau_0 \sim 1$), an estimate of its size. Such an estimate is inaccessible to analysis restricted only to spectral fits or simply to measurements of the PSDs. Therefore, if the high-energy radiation is produced in the vicinity of the compact object and the observed PSDs are due to a modulation of the accretion rate by a hitherto unknown process, as most models contend (see, e.g., Chen & Taam 1995; Takeuchi, Mineshige, & Negoro 1995), these lags should be roughly of the order ~ 1 ms or shorter, the electron scattering time near the compact object, independent of the modulation of overall fluctuations of the light curve.

Motivated by the above considerations and the apparent discrepancy between the observed and expected variability timescales of BHCs, we have recently embarked on a study of the timing properties of inhomogeneous, hot electron clouds of significant spatial extent. Our goal in this effort was to provide models for the light curves and other timing properties (PSD, lags) of BHCs that would attribute some physical significance to the features of their PSDs discussed above. Thus in Kazanas, Hua, & Titarchuk (1997; hereafter KHT) we have studied the time response of such extended sources and indicated that the observed PSD could be understood as resulting from Comptonization of soft photons by hot electron configurations that extend over several orders of magnitude in radius, identifying the break at ν_c in the PSD with the "outer edge" of the scattering cloud. In Hua, Kazanas, & Titarchuk (1997; hereafter HKT) we examined the coherence function (hereafter CF; Vaughan & Nowak 1997) associated with such spatially extended hot electron configurations and indicated that, because of the linearity of the Comptonization process, these configurations are expected to exhibit a high degree of coherence as well as long hard X-ray lags, in agreement with observations. More recently, Kazanas & Hua (1998) have produced model light curves associated with these configurations and studied their properties in the time domain, using moments of various orders which they then correlate with other observables.

In the present work we focus our attention to a more detailed study of the lags between different bands of the X-ray light curves. In § 2 we collect all the lag and spectral observations associated with the light curves of BHCs, which we were able to obtain in the literature; we indicate that these lags have a form that appears to be very similar among these different sources and that does not correlate in an obvious way with their well-studied spectral states, and we provide fits to the observed lags using our earlier models. In § 3 we provide a heuristic account of the form of the observed lags and their dependence on the density distribution of the hot Comptonizing electrons, as well as models that allow one to compute the form of lags analytically, thus making transparent their origin. In § 4 we demonstrate by direct numerical simulation the dependence of the lag form on both the spatial distribution of Comptonizing electrons and the location of the source of soft photons, and we provide the form of the lags associated with a variety of such configurations. Finally, in § 5 the results are summarized, and conclusions are drawn.

2. THE LAG OBSERVATIONS

As indicated in the introduction, the need for models with timing properties that are in agreement with the observations of the PSDs and the hard X-ray lags of BHCs motivated KHT to study the timing properties of the Comptonization process by *inhomogeneous*, *extended*, hot electron configurations of the form

$$n(r) = \begin{cases} n_i & \text{for } r \le r_1 \,, \\ n_1 (r_1/r)^p & \text{for } r_2 > r > r_1 \,, \end{cases} \qquad (2)$$

where the power index p is a free parameter, r is the radial distance from the center of the spherical corona, r_1 and r_2 are the radii of its inner and outer edges, respectively. Note

that the density of the central uniform core, n_i, does not necessarily join smoothly to that of the extended corona. It is apparent that the density profile of equation (2) allows Compton scattering to take place over a wide range of densities, thereby introducing time lags over a similar range of timescales and at the same time producing variability over a similar frequency range, thus providing a straightforward account and physical significance to the observed PSDs (KHT).

In Figure 1 we present the time lags associated with the *Ginga* observations of Cyg X-1 in 1987 August, when the source was apparently in its *hard* state, as reported by Miyamoto et al. (1988). On the same figure we also plot the times lags associated with a variety of electron configurations of the general form of equation (2), as computed using the Monte Carlo code of Hua (1997). These were computed by injecting the soft photons at $r = 0$ from a black body distribution of $kT_r = 0.2$ keV to an electron cloud with temperature $kT_e = 100$ keV and Thomson depth $\tau_0 = 1$. The escaping photons were collected according to their arrival time to the observer as well as their energy. The energy bins used were 15.8–24.4 and 1.2–5.75 keV, in order to be directly compared to the observational data. In each energy bin, the photons were collected into 4096 time bins over 16 s, each 1/256 s in length. The light curves so obtained were then used to calculate the time lags of the emission in the higher energy bin with respect to that in the lower one.

The time lags resulting from Comptonization of the soft photons a uniform corona (Fig. 1; *dotted curve*) were obtained by further setting its density to $n = 10^{16}$ cm^{-3}. It is seen that the lags are constant ≈ 2 ms down to a period ~ 0.005 s and then decrease at smaller periods. This is because for emission from such a corona the hard X-ray lags are due to scatterings in a region with a mean free time of the order $0.3/n\sigma_T c \simeq 1.5$ ms (Hua & Titarchuk 1996). The magnitude of the time lag reflects this characteristic time. The dot-dashed curve represents the lag form for a uniform source of the above density obtained using the analytic formula of Payne (1980). The difference in the lag normalization is indicative of the corrections introduced by using the Klein-Nishina, as opposed to the Thomson, cross section used in the analytic formula in the scattering time expression. The solid line represents the lags corresponding to a corona with $p = 1, n_i = n_1 \sim 10^{16}$ cm^{-3}, $r_1 = 10^{-3}$ lt-s, $r_2 = 10^3 r_1$, and electron temperature 100 keV. This curve has a linear dependence on the Fourier period ranging from $P = 0.03$ s up to ~ 3 s. There is a cutoff at the periods below $P = 0.03$ s due to the finite time resolution of our calculation. At periods $P \gtrsim 4$ s the curve levels off, indicating that the time lag of hard X-ray reaches its maximum of ~ 0.1 s. The wide range of the lags reflects the fact that the scatterings take place in a region with densities ranging from $\sim 10^{16}$ to 10^{12} cm^{-3}. The time lags resulting from the corona with $p = \frac{3}{2}$ density profile are represented by the dashed curve. It is seen that dependence of lag on period is weaker and the maximum time lag is only $\sim 10^{-2}$ s, indicating that, although the corona extends to a radius of ~ 1 lt-s, there is virtually no photon scattering beyond a radius $\sim 10^{-2}$ lt-s because of the steep density gradient. A calculation based on the density profile of equation (2) indicates that the optical depth of the corona for $r > 10^{-2}$ lt-s is $\sim 7.5\%$ of the total depth for $p = \frac{3}{2}$, while in the case of $p = 1$, the corresponding percentage is 40%.

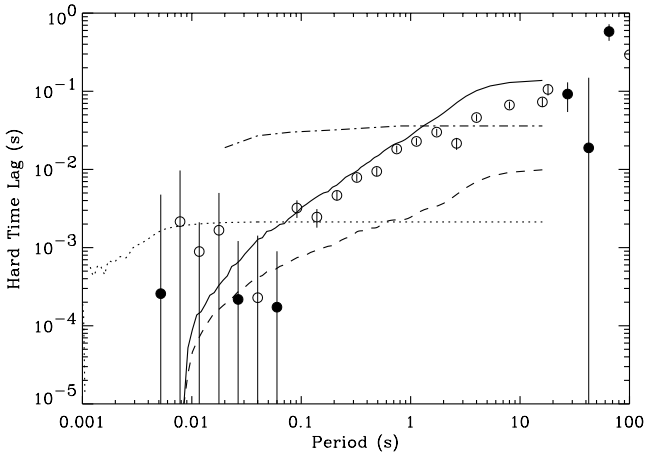

FIG. 1.—Time lags of hard X-rays (15.8–24.4 keV) with respect to soft ones (1.2–5.7 keV) as a function of Fourier period, obtained from the analysis of *Ginga* data of Cyg X-1 (Miyamoto et al. 1988). The circles and dots represent the measured positive and negative lags, respectively. The dash-dotted curve represents the lag predicted based on analytical Comptonization model given in Miyamoto et al. (1988) and assumed corona electron density 10^{16} cm^{-3}. The three other curves are calculation results for Comptonization in the model coronae that produce the energy spectra shown in Fig. 2.

One should note that our choice of τ_0 and T_e above was rather arbitrary. However, the values of these parameters can be meaningfully constrained from fits of the corresponding spectra of these sources. In order to display in detail the constraints imposed by the combined spectral-temporal analysis of the BHC data, we now present fits of both the spectra and the corresponding lags associated with the observations of Cyg X-1 by Cui et al. (1997a, 1997b). As an example, we here use their results from observation 6, when the source was in its high (soft) state, whereas the other two reported sets of data in the above references were from observations 3 and 15, during which the source was in a transition between its soft and hard states.

In Figure 2 we have plotted the Proportional Counter Array (PCA; *circles*) and High-Energy X-Ray Timing Experiment (HEXTE; *dots*) data covering an energy range 2–200 keV from *Rossi X-Ray Timing Explorer* (*RXTE*) observations of Cyg X-1 in its 1996 high state (Cui et al. 1997a). On the same figure, in order to provide the tightest possible constraints to our models, we have also plotted the Burst and Transient Source Experiment (BATSE) data obtained by Ling et al. (1997) 2 yr earlier while the source was in a similar high (soft) state, referred to by Ling et al. (1997) as the γ_0 state. By definition, in the high state, the soft ($\lesssim 10$ keV) X-ray flux is high relative to the hard ($\gtrsim 30$ keV) flux. Such a distinct anticorrelation between the soft and hard bands was confirmed by the simultaneous monitoring of Cyg X-1 with the All-Sky Monitor (ASM)/*RXTE* and BATSE (Cui et al. 1997a; Zhang et al. 1996). Because the BATSE observations of Ling et al. (1997) were indeed obtained during such a high state (note the almost identical fluxes between HEXTE and BATSE in the overlap energy range: the small difference could be attributed to uncertainties in the cross calibration between HEXTE and BATSE), we speculate that the state of the source was not very different in these two observations, even though no simultaneous coverage of its soft energy band was at the time available (in any case these observations are served to *constrain* rather than facilitate the fits of our models).

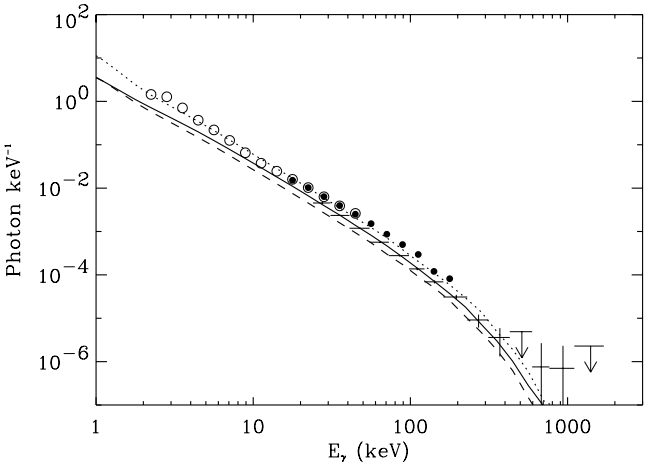

FIG. 2.—Three calculated energy spectra that fit equally well the Cyg X-1 data (*crosses*) in its γ_0 state observed by *CGRO*/BATSE in 1994 (Ling et al. 1997). These spectra result from Comptonization in coronae with the same temperature but different optical depths and density profiles: $p = 0, \tau_0 = 0.5$ (*dotted line*), $p = 1$, $\tau_0 = 1.0$ (*solid line*), and $p = \frac{3}{2}$, $\tau_0 = 0.7$ (*dashed line*). The dotted and dashed curves are slightly displaced to separate the otherwise nearly identical curves. Also plotted are *RXTE*/PCA (*circles*) and HEXTE (*dots*) data from the same source observed during its high state in 1996 (Cui et al. 1997a).

In Figure 3 we have plotted the time lags between the energy bands 13–60 keV and 2–6.5 keV corresponding to the above data set (i.e., of observation 6) as a function of the Fourier period, with the data points regrouped into logarithmically uniform bins in Fourier period. A linear dependence of the lag on the Fourier period in the range $P \sim 0.03$–3 s is evident as in the *Ginga* data of Miyamoto et al. (1988).

In both Figures 2 and 3 we present, in addition to the data, model fits to the spectra (in Fig. 2) and the associated lags (in Fig. 3) corresponding to configurations of different values of the parameter p. Thus the solid lines in both figures correspond to coronae with $p = 1$, the dashed lines to $p = \frac{3}{2}$, while the dotted ones to a uniform distribution ($p = 0$). The temperature of the plasma was taken to be $kT_e = 100$ keV. The rest of the parameters of the configurations are as follows: (1) For $p = 1$, $n_i = n_1 = 4.35 \times 10^{16}$ cm^{-3}, $r_1 = 10^{-4}$ lt-s, with a Thomson depth $\tau_i = 0.2$. The total optical depth of the corona is $\tau_0 = 1$. (2) For $p = \frac{3}{2}$, $n_1 = 1.6 \times 10^{17}$ cm^{-3}. Its uniform inner core has the same radius as the $p = 1$ case, but a Thomson optical depth $\tau_i = 0.07$. (3) For $p = 0$, $n = 10^{16}$ cm^{-3}, and $\tau_0 = 0.5$, leading to $r_2 \simeq 7.5 \times 10^7$ cm.

It is seen that over the energy range 20–200 keV, the spectra corresponding to $p = 1$ and $\frac{3}{2}$ are almost identical to those of the $p = 0$ configuration (Fig. 2; *dotted curve*). In fact, their χ^2 values are 7.8 and 8.1, respectively (with 8 degrees of freedom), comparable to that of the uniform source. In other words, these three models provide equally good spectral fits to the data, an argument made from a purely theoretical point of view also in KHT. One should note, however, that the total Thomson depths of the corresponding configurations are indeed different in these three cases. On the other hand, the differences in the lags corresponding to these three configurations are too apparent to require statistical analysis. The shapes of the curves are similar to those in Figure 1, but the magnitudes of the lags are slightly smaller, because of the smaller gap between the reference energy bands in this case. Obviously, the corona with $p = 1$ is again favored by the observation.

Similar lag analyses have been performed for a number of BHC sources in a small number of observing epochs (compared to those of spectral analyses of the same sources). Thus analysis of the light curves of the source GX 339−4 obtained by *Ginga* (Miyamoto et al. 1991) and the source GRS 1758−258 obtained by *RXTE* (Smith et al. 1997; Fig. 4) have indicated a similar linear dependence of the lags on the Fourier period. In the latter case, the time lags of hard X-rays (6–28 keV) with respect to soft ones (2–6 keV) extend to $\delta t \simeq 1$ s for $\nu \sim 0.02$ Hz! In Figure 5, we present the lags associated with the high-energy transient source GRO J0422+32, which was observed by *Compton Gamma-Ray Observatory* (*CGRO*)/OSSE during outburst. Analysis of the associated lags between the hard (75–175 keV) and soft X-rays (35–60 keV) in this data set, indicated a similar behavior (Grove et al. 1997, 1998) over the Fourier period range $P \sim 0.1$–100 s. The time lags level off at $\omega \sim 0.025$ Hz after reaching a value of ~ 0.3 s. In Figure 5 we provide a tentative fit to these data obtained from a calculation based on Comptonization in a model corona

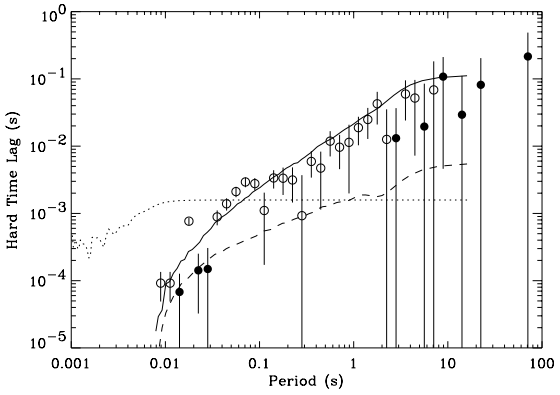

FIG. 3.—Time lags of hard X-rays (13–60 keV) with respect to soft ones (2–6.5 keV) resulting from Comptonization in the same coronae that produce the energy spectra shown in Fig. 2. The dotted, solid, and dashed curves, as in Fig. 2, represent the density profiles $p = 0$, 1, and $\frac{3}{2}$, respectively. The time lag between the same energy bands based on *RXTE* data from Cyg X-1 (Cui et al. 1997b) are also plotted in the figure.

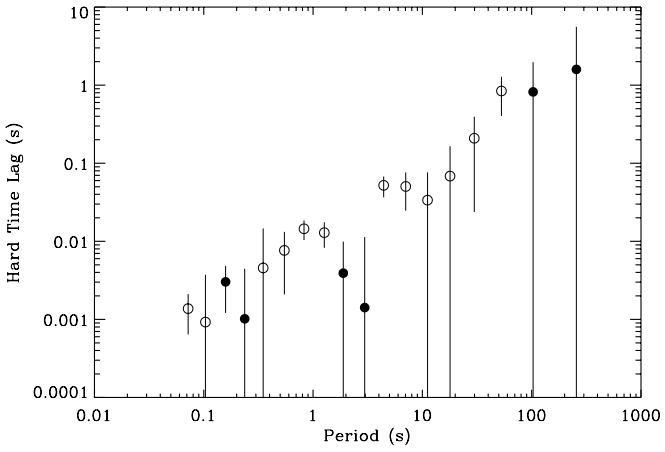

FIG. 4.—Time lags of hard X-rays (6–28 keV) with respect to soft ones (2–6 keV) as a function of Fourier period for the source GRS 1758−258. This is converted from the phase lag vs. frequency relation obtained by Smith et al. (1997). Dots are negative lags.

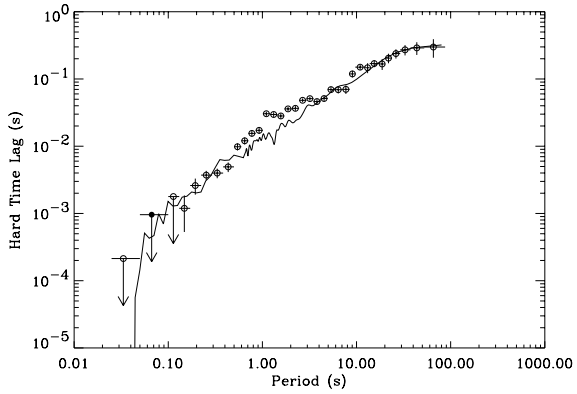

FIG. 5.—Time lags of hard X-rays (75–175 keV) with respect to soft ones (35–60 keV) as a function of Fourier period for the source GRO J0422+32, obtained by Grove et al. (1997) from OSSE observation. The solid curve is obtained from a calculation based on Comptonization in a model corona with $p = 1$, $r_2 = 1.9 \times 10^{11}$ cm, $kT_e = 100$ keV, and $\tau_0 = 0.25$.

with $p = 1$, $kT_e = 100$ keV, $\tau_0 = 0.25$, $n_1 = 2.5 \times 10^{15}$ cm^{-3}, $r_1 = 4.8 \times 10^{-4}$, and $r_2 = 6.4$ lt-s. Although these parameters can be determined unequivocally only by fitting the simultaneous spectral and temporal data, the discussion in § 3 will show that at least the parameters p and r_2 can be estimated with the lag observation alone. Particularly, r_2 of the model corona can be estimated from the equation

$$r_2 \sim P_c/2\pi \,, \tag{3}$$

where P_c is the period at which the lag curve levels off, $\simeq 40$ s in this particular case. These results suggest that the frequency-dependent hard X-ray time lags may be a common property of these sources at least during particular states of their emission.

While the data presented so far seem to favor Comptonization in coronae with $p = 1$, there are indications of a density profile with $p = \frac{3}{2}$ in the recent Cyg X-1 data in its low (hard) state (Wilms et al. 1997) and during the transition states (Cui et al. 1997b). In Figure 6 we display the time lags of hard (14.09–100 keV) with respect to soft (0–3.86 keV) X-rays based on the *RXTE* data reported by Wilms et al. (1997). We also plot the time lags (*solid curve*) resulting from a calculation of Comptonization in a model corona with $p = \frac{3}{2}$, $kT_e = 100$ keV, $\tau_0 = 1.5$, $n_1 = 2.53 \times 10^{16}$ cm^{-3}, $r_1 = 0.001$, and $r_2 = 5$ lt-s. While we need the simultaneous spectral data in order to determine the values of T_e and τ_0, it is clear that the density profile with $p = \frac{3}{2}$ does provide a valid fit to the lag data, independent of the particular spectral fit.

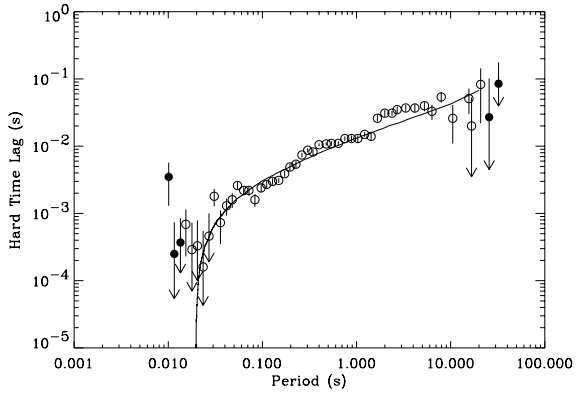

FIG. 6.—Time lags of hard X-rays (14.09–100 keV) with respect to soft ones (0–3.86 keV) as a function of Fourier period for the source Cyg X-1 based on *RXTE* data (Wilms et al. 1997). The solid curve is a result from the calculation of Comptonization in a corona with $p = \frac{3}{2}$, $kT_e = 100$ keV, $\tau_0 = 1.5$, and $r_2 = 5$ lt-s.

More recently, Crary et al. (1998) reported the hard X-ray lags of Cyg X-1 observed by *CGRO*/BATSE during a period of approximately 2000 days. The time lags are between the energy bands 50–100 keV and 20–50 keV over the Fourier period ranging from $P \gtrsim 5$ s to as large as ~ 130 s. Again, the lags are frequency dependent, obeying the relation $\delta t \propto \omega^{-0.8}$. As we have seen in the Figures 1, 3, and 6, both density profiles $p = 1$ and $\frac{3}{2}$ will lead to lags of the form $\delta t \propto \omega^{-q}$ with $q \simeq 1$ and 0.6, respectively. Since the result of Crary et al. (1998) is an average over a very long time span, it is not unreasonable to speculate that during this time the density profile of the corona in Cyg X-1 evolved between the configurations with $p = 1$ and $\frac{3}{2}$. This data set has extended the lag determination to the longest Fourier period to date and discovered X-ray lags rising almost out to this Fourier period. According to equation (3), this result, if confirmed, implies an exceptionally large outer edge for the Comptonizing corona (~ 20 lt-s!).

3. THE COMPUTATION OF LAGS

As indicated in the explicit examples and fits to the data given in the previous section, the information associated with the lags is largely independent of that of the spectra and is necessary for providing a complete description of the structure of Comptonizing sources, an issue to which spectral fits can contribute very little. The power spectra can also provide information about the structure of the sources; however, because their form can be affected by the modulation of the accretion rate (see end of this section), this information is not unequivocal.

The lags associated with the light curves in two different energy bands are essentially the *average* of the difference of the paths lengths (divided by c) followed by photons in the two different energy bands, the photons of larger energy having spent longer in the hot plasma. For a uniform source, this difference is (roughly) some fraction of the scattering time of the photons in the medium (Payne 1980), and for media of small Thomson depth, $\tau_0 \sim 1$, it is of order of a fraction of the light crossing time of the scattering region. Since the size R of this region corresponds to a particular Fourier period $P \sim R/c$, in principle, lags of all periods P are present in sources with any type of spatial density distribution. What distinguishes the form of lags in sources with different spatial density profiles is the additional probability of scattering within a region of a given size R, $\mathscr{P}(R)$. Thus, for a uniform density configuration, $\mathscr{P}(R) \propto R$ (for $R < r_2$; r_2 is the outer edge of the corona), leading to lags of the form $\delta t \propto [\mathscr{P}(R)]R \propto R^2 \propto P^2$ for $P \lesssim r_2/c$; the lags become constant for larger periods, since no further scattering takes place at longer timescales (larger radii). For $p = 1$, $\mathscr{P}(R) \simeq$ constant, leading to lags $\delta t \propto P$ as indicated by our simulations, while for $p = \frac{3}{2}$, $\mathscr{P}(R) \propto R^{-1/2}$, leading to $\delta t \propto P^{1/2}$, again in agreement with the results of our Monte Carlo simulations presented in the figures above.

One should note that a conclusion following from the above arguments is that the *form* of the lags as a function of

Fourier period under the conditions discussed above—i.e., constant electron temperature and injection of the soft photons near the center of the corona—depends mainly on the probability of photon scattering within a given range of radii. Therefore, the lag dependence on the Fourier period P is characteristic of the electron density profile alone, and, in our opinion, it could serve as a probe of it. The reader should note the distinct difference in information content between the lags and the spectrum: the latter depends simply on the total probability of scattering through the entire corona, while the former on the differential probability of scattering within a given range of radii. Because the lags are simply a manifestation of the difference in average path of photons in two different energies, they also depend on the position of the photon source, as will be exhibited through a number of examples in the next section.

The dependence of the lags on the Fourier period associated with the plasma configurations discussed in the previous section and depicted in the appropriate figures can be derived more formally using the Green's function of the associated problem, i.e., the form of the high-energy light curves in response to an instantaneous input of soft photons at their center. In KHT, it was shown by numerical simulation that the Green's function of this problem for a configuration with $p = 1$ has a power-law shape, with an index close to -1 that becomes flatter with increasing total Thomson depth and photon energy. In both cases there is a cutoff corresponding to the timescale, β, characteristic of the photon escape time from the system. These light curves can be approximated fairly well analytically by the gamma function distribution,

$$g(t) = \begin{cases} t^{\alpha-1}e^{-t/\beta}, & \text{if } t \geq 0, \\ 0, & \text{otherwise}, \end{cases} \tag{4}$$

where t is time and $\alpha > 0$ and $\beta > 0$ are parameters determining the shape of these light curves.

The light curves from a uniform electron corona correspond to $\alpha \simeq 1$ so that the gamma distribution function reduces to an exponential. Because the hot electron configuration in this case is assumed to be confined to the vicinity of the compact object, the corresponding value for β is assumed to be of order 10^{-3} s, although more extended uniform configurations can in principle be analyzed by letting the value of this parameter be proportionally larger. A corona with density profile corresponding to $p > 0$ is inhomogeneous, and the properties related to this specific characteristic manifest for large values of the ratio of its inner and outer radii r_2/r_1. Motivated by these observations we require $r_2 \sim 1$ lt- s, which corresponds to $\beta \sim 1$ s with a value for α small compared to 1. The Fourier transform of the function $g(t)$ is

$$G(\omega) = \frac{\Gamma(\alpha)\beta^{\alpha}}{\sqrt{2\pi}}(1 + \beta^2\omega^2)^{-\alpha/2}e^{i\alpha\theta}, \tag{5}$$

where $\Gamma(x)$ is the gamma function and $\omega = 2\pi\nu = 2\pi/P$ is the Fourier circular frequency; θ is the phase angle that we are interested in and is given by

$$\tan\theta = \beta\omega. \tag{6}$$

If we consider two light curves in two energy bands distinguished by different values of α and β—say α_1, β_1, and α_2, β_2—the time lag between them will be given by their phase lag θ divided by the corresponding frequency ω; i.e.,

$$\delta t = \frac{1}{\omega}[\alpha_2 \arctan(\beta_2\omega) - \alpha_1 \arctan(\beta_1\omega)]. \tag{7}$$

For large periods P (small ω) or $\beta_1\omega$, $\beta_2\omega \ll 1$, δt approaches the constant $\alpha_2\beta_2 - \alpha_1\beta_1$. On the other hand, for small P or $\beta\omega \gg 1$, $\delta t \simeq (\alpha_2 - \alpha_1)P/4$. In the case of a uniform corona for which $\alpha_2 = \alpha_1 = \alpha \simeq 1$, expanding equation (7) to higher order in ω, we obtain $\delta t \propto \alpha(1/\beta_1 - 1/\beta_2)P^2$. The transition from latter to the former occurs at

$$\beta\omega \sim 1 \quad \text{or} \quad P_c \sim 2\pi\beta. \tag{8}$$

This immediately gives equation (3) if we remember that the outer radius r_2 is of the same order as β.

The analytic results presented above are given in graphic form in Figures 7*a* and 7*b*. In Figure 7*a*, we plot two pairs of light curves associated with the function $g(t)$, one with $\alpha_1 = 0.1$, $\alpha_2 = 0.2$, $\beta_1 = 1$, and $\beta_2 = 1.25$, the other with $\alpha_1 = \alpha_2 = 1.0$, $\beta_1 = 0.001$, and $\beta_2 = 0.0025$. The former represents the light curves resulting from a corona with $p = 1$ density profile and $r_2 \simeq 1$ lt-s, while the latter is from a uniform one with $r_2 \simeq 10^{-3}$ lt-s. The time lags between these two pairs of light curves are computed as indicated

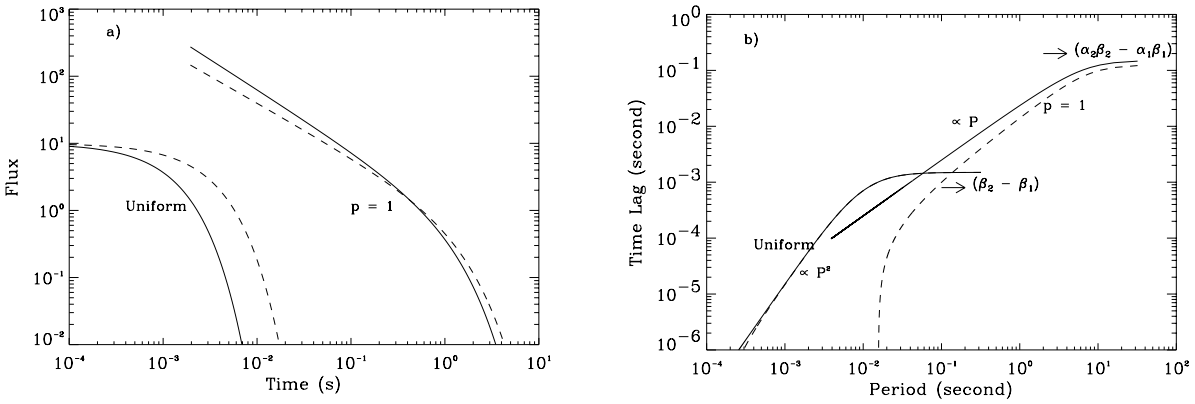

FIG. 7.—(*a*) Two pairs of light curves corresponding to two sets of values of α and β in eq. (2). The pair with $p = 1$ represents the light curves from a cloud with $1/r$ density profile, and the other pair are from a cloud with a uniform one. The solid curves correspond to the light curves in the lower energy bands. (*b*) Time lags based on eq. (7) between the two curves in each pair in Fig. 7. The dashed curves are times lags obtained by numerical Fourier transformation with finite time resolution.

above and presented in Figure 7*b*. The dependence of the lag shape to the parameters α and β is apparent in these figures: For pure exponential light curves $\alpha = 1$ (or, more precisely, for light curves with $\alpha_1 = \alpha_2$), the time lag is proportional to P^2 for $P < P_c \simeq 0.006$ s and turns to a constant value for larger P, whereas the value of the lags at this point is of order $\beta_2 - \beta_1 \simeq 1$ ms. For the curves with $0 < \alpha < 1$, the time lag is proportional to P for $P < P_c \simeq 6$ s and turns to a constant for large P. In both cases, the level-off point is $P_c \simeq 2\pi\beta$ with the value of β appropriate for each case; however, the time lag resulting from the purely exponential light curves has no portion linear in P. Thus the existence of a linear portion in the time lag curves obtained from fits to observations clearly favors light curves that include power law sections such as those of equation (4). As discussed in KHT, such a form for the response functions is a signature of a nonuniform density distribution of the Comptonizing corona, and the values of α and β are closely related to the physical size and density distribution of the source corona.

Having obtained the Fourier transform $G(\omega)$ (eq. [5]) of the light curve $g(t)$ (eq. [4]), one can easily compute the Fourier transform associated with a light curve consisting of the sum of two such light curves separated by an interval t_0, i.e., the light curve $g_1(t) = g(t) + g(t - t_0)$. According to the well-known Fourier analysis theorems, this will consist of the sum $G(\omega) + G_0(\omega)$, with $G_0(\omega) = G(\omega)e^{i\omega t_0}$. Therefore, the presence of the additional shot induces only a change in the *phase* of the corresponding Fourier transform, the latter becoming $\theta + \omega t_0$. Since the change in phase associated with the second light curve, $g(t - t_0)$, is the same for photons that belong in two different energy bands (the light curve of each band is shifted by t_0), their *phase difference* and hence their time lags are unaffected by the presence of additional shots. Considering that any light curve $f(t)$ can be written as the convolution of $g(t)$ with a modulating function $M(t)$, by the arguments given above, such modulation will not affect the *phase differences* and hence the time lags between two different energy bands. However, it will have a great impact on the resulting power spectra, which now are proportional to $|M(\omega)G(\omega)|^2$, where $M(\omega)$ is the Fourier transform of $M(t)$.

It becomes apparent, therefore, that the additive nature of the phases associated with the Comptonization process makes phase differences, and hence the corresponding time lags, immune to any particular modulation of the rate at which matter is accreted onto the compact object. As such, they map out properties that are inherent to the Comptonizing hot electron plasma rather than to the modulation of the accretion rate (usually invoked to account for the PSD), in as much as the latter does not change the plasma's overall properties significantly. In this respect, Miller (1995) has argued that oscillations of the scattering corona do preserve the phase relations established by the Comptonization process, provided that their period of oscillation is longer than the scattering time responsible for the formation of the lags. Our point of view in the present note is slightly different: in our simple models we posit that the observed lags are in fact produced by scattering in the corona and that their magnitude provides an estimate of its size. The sizes thus deduced by our models are much larger ($\lesssim 10^{11}$ cm) than the size of the horizon of the putative black hole, where presumably most of the accretion energy is converted in radiation; this discrepancy between the estimated (through the lag measurements) and the expected (on energetic arguments) sizes of the X-ray–emitting region is precisely the controversial aspect of the observed lags. In an attempt to ameliorate this discrepancy, Nowak et al. (1997) have proposed models of waves propagating inward in the accretion disks near the compact object, which at the same time are associated with radiation emission. They further postulated that the emitted radiation becomes hotter at smaller radii, thus giving rise to lags between soft and hard X-rays. As the authors themselves point out, the problem with this type of model is that the wave speeds needed to produce lags of the observed magnitude are $c_s \simeq 0.01c$, i.e., much slower than those typical of the dynamics or radiation transfer in this region. It is also not obvious whether such waves, if of random phases, would yield the high values of the CF observed in this class of sources (see next paragraph). Therefore, in either way, the size of the observed lags indicates that some of our cherished notions concerning the structure and dynamics of these objects are drastically incorrect.

The properties of the Comptonizing coronae are generally expected to be time-variable, and their variability should have some effects on the corresponding phases. The issue of the preservation of phases in time-varying coronae is to a large degree related to the observed high values of the CF of the light curves of accretion powered high-energy sources (see Vaughan & Nowak 1997; HKT), which effectively is the normalized cross spectrum at two different energy bands averaged over the duration of the observation. As argued in HKT, the linearity of the Comptonization process leads naturally to high values ($\simeq 1$) for the CF in plasmas with parameters that do not change in the duration of observation. HKT have explored the dependence of CF on variations in the plasma temperature T_e; as shown in their Figure 2, changes in T_e by a factor of 2 over the duration of observation lead to a uniform decrease in the value of the CF (CF $\simeq 0.8$ as opposed to CF $\simeq 1$ for a constant T_e) over the entire 0.1–100 Hz frequency range. This uniformity in the CF decrement is indicative of the fact that the relative sign of the phases is rather well preserved despite the change in the electron temperature (this last statement depends on the energy bands used in the computing the CF; in HKT they were both below the minimum temperature attained by the electrons in the course of the variation of their temperature). Observations indicating CF $\simeq 1$ (Vaughan & Nowak 1997; Nowak et al. 1997) strongly suggest that the temperature of the scattering plasma has remained constant over the entire observation interval.

Thus, under the assumptions of the present calculations (i.e., Comptonization as the main process of high-energy emission, uniform temperature, nonuniform density, and central soft photon injection), the time dependence of the photon flux, i.e., the light curves, at various energies can be used to determine the size of the hot electron corona and map its radial density distribution (i.e., determine the index p). This fact provides the possibility of deconvolution of the density structure of these coronae through a combined spectral-timing analysis similar to that indicated above.

4. LAGS AND THE SOFT PHOTON SOURCE LOCATION

In the previous section we discussed the general notions associated with lags induced by Comptonization in inhomogeneous media of spherical symmetry and their dependence on the Fourier period, which was derived both

heuristically and formally for specific cases. It was also argued that the form of the lags so derived and exhibited in Figures 1, 3, 4, 5, and 6 depends, in addition, on the assumption that the injection of the soft photons takes place near the center of the hot, spherical electron configuration. It is easy to see that if the latter assumption is not true the resulting lags could have different form than those computed above; if the source is of finite extent or not located at the center, the scaling concerning the probability of photon scattering at a given range of radii would be different from that given above, leading to different scaling of the lags as a function of Fourier period. It is hence conceivable, under these conditions (extended or noncentral soft photon source) and if the coronae are optically thin, that one could receive soft photons emitted from the farther edge of the soft photon source at a later time than photons originating in its near side, which did increase their energy by scattering on the way to the observer, thereby introducing negative lags in the system. The effects of a centrally located source of finite extent $r_{\rm in}$ were discussed in HKT, where it was pointed out that it would lead to loss of coherence on timescales $r_{\rm in}/c$. This loss of coherence is generally manifest with the presence of negative lags in the appropriate Fourier frequency range.

Therefore the form of the observed lags conveys information not only about the density distribution of the hot electrons but also about the distribution of the source of soft photons. The effects of the finite distribution of the soft photon source manifest in the loss of coherence of the scattering medium over the periods appropriate to the light crossing time of the soft photon source, as discussed in HKT. In this section we present the lags corresponding to a number of arrangements different from those examined heretofore in order to substantiate the above arguments and to exhibit the form of the lags in certain geometries that are favored by popular models of these sources.

We therefore consider the location of the soft photon source to be *external* to the hot, spherically symmetric cloud and arranged in a ring geometry of finite width and inner radius $r_{\rm in} = 4$ lt-s in order to simulate injection of soft photons by an outlying cool accretion disk. The hot electron cloud responsible for the Comptonization is assumed to be spherically symmetric, centered at $r = 0$, with electron temperature $T_e = 100$ keV, outer radius $r_2 = 1$ lt-s, and total Thomson depth $\tau_0 = 1$. We further consider two different cases for the density distribution of the hot electrons: (1) A corona with $p = 0$ (uniform) and density $n = 1.5 \times 10^{13}$ cm^{-3}, and (2) a corona with a $p = 1$ density profile, an inner radius $r_1 = 1.25 \times 10^{-4}$ lt-s, and a density $n_1 = 4 \times 10^{16}$ cm^{-3}. We also consider two different cases for the outer radius of the ring, $r_{\rm out} = 4.001$ and 4.5 lt-s, respectively, in order to study the effects of the finite size of soft photons on the structure of the lags. The soft photons are drawn from a black body distribution of temperature $T_r = 1$ keV, while the lags are computed among the following energy bands: 1–5 keV (band 1), 5–10 keV (band 2), and 10–50 keV (band 3).

In Figures 8, 9, 10, and 11 we present the results of our simulations. Figures with the subscript *a* exhibit the form of the light curves for the different energy bands indicated above, while figures of subscript *b* show the corresponding lags between the marked pairs of energy bands. In Figures 8*a* and 8*b* we present the results for a corona with $p = 1$ and a soft photon source of $r_{\rm out} = 4.001$ lt-s. Figures 9*a* and 9*b* show the results of a uniform corona ($p = 0$) and soft photon source of $r_{\rm out} = 4.001$ lt-s. Figures 10*a* and 10*b* show the results for a corona with $p = 1$ and soft photon source of $r_{\rm out} = 4.5$ lt-s. Figures 11*a* and 11*b* show the results for a uniform corona and a soft photon source of $r_{\rm out} = 4.5$ lt-s.

The consistency of our results has been tested by reproducing with high accuracy the analytic results of the previous section for the case of central soft photon injection both for a uniform and a $p = 1$ corona. The light curves were derived by employing the Monte Carlo code of Hua (1997) with 10^7 photons run^{-1} and collecting the photons emerging from the hot electron cloud in all directions; the lags were subsequently computed from these light curves, as discussed in the previous section.

The light curves of Figures 8*a* and 9*a* exhibit a sharp peak at times near $t = 2$ s for bands 1 and 2. These are due to photons that traversed the entire length of the corona, through its center, exiting on the opposite side with only a small gain in energy. The photons in band 3, having suffered a larger number of scatterings, have apparently followed

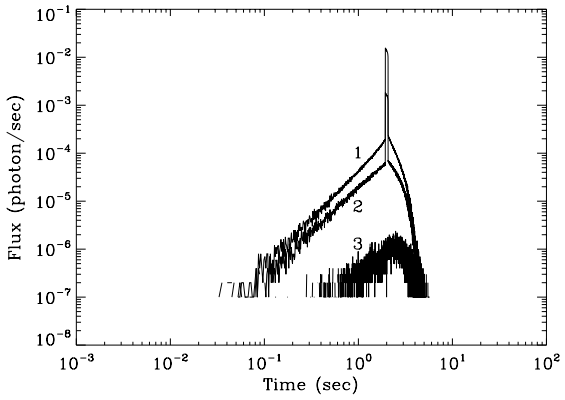

FIG. 8*a*

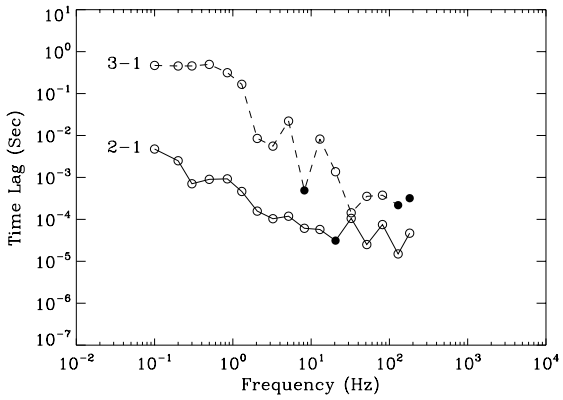

FIG. 8*b*

FIG. 8.—(a) Light curves corresponding to 3 energy bands (band 1, 1–5 keV; band 2, 5–10 keV; band 3, 10–50 keV) as marked on the figure for a soft photon source exterior to the hot electron cloud. The source is located on a ring of radii $r_{\rm in} = 4.0$, $r_{\rm out} = 4.001$ lt-s. The hot electron corona is concentric to the ring with an electron temperature $T_e = 100$ keV, total Thomson depth $\tau_0 = 1$, and outer radius $r_2 = 1$ lt-s. It has a density profile with $p = 1, r_1 = 1.25 \times 10^{-4}$ lt-s, and $n_1 = 4 \times 10^{16}$ cm^{-3}. (*b*) Lags as a function of Fourier frequency between bands 3, 1 and 2, 1 as marked on the figure for the configuration corresponding to (*a*).

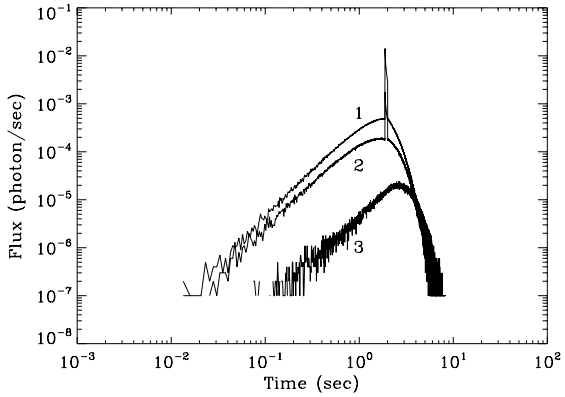

FIG. 9*a*

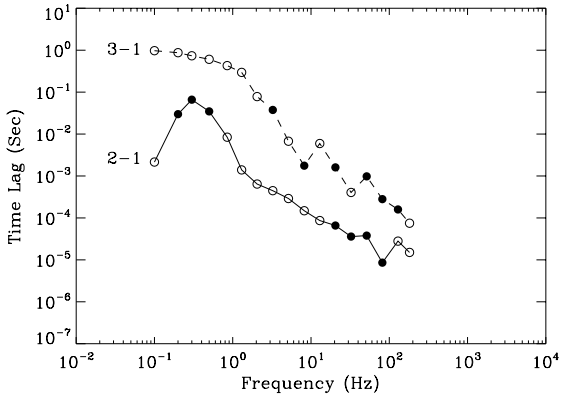

FIG. 9*b*

FIG. 9.—(*a*) Same configuration and parameters as for Fig. 8*a* except for a uniform corona ($p = 0$) of $n = n_1 = 5 \times 10^{13}$ cm^{-3}. (*b*) Same as in Fig. 8*b* for the configuration corresponding to (*a*).

very different paths and hence do not exhibit this feature. The corresponding lags are given in Figures 8*b* and 9*b*, marked by the energy bands involved; they are of apparently different form than those obtained from central injection of soft photons. Their magnitude is also smaller than that obtained in our Figures 1–6 of the previous section, with the exception of the lags between bands 3 and 1 in the lowest frequencies ($\lesssim 1$ Hz), which are indeed commensurate with the light crossing time through the corona. Of interest is also the presence of some *negative* lags (*filled circles*) at certain frequency ranges, possibly related to some backscattered photons. The general dependence of lags on Fourier frequency in these two cases is also different from that associated with central soft photon injection, although

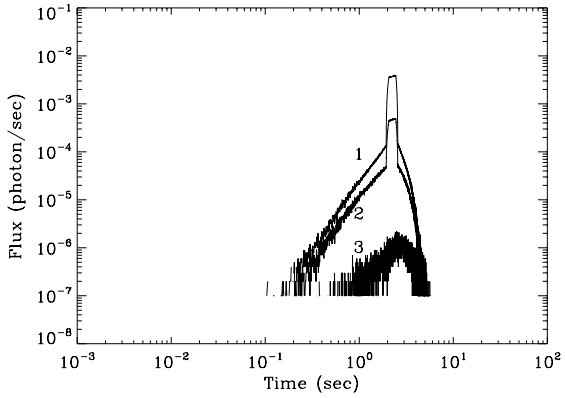

FIG. 10*a*

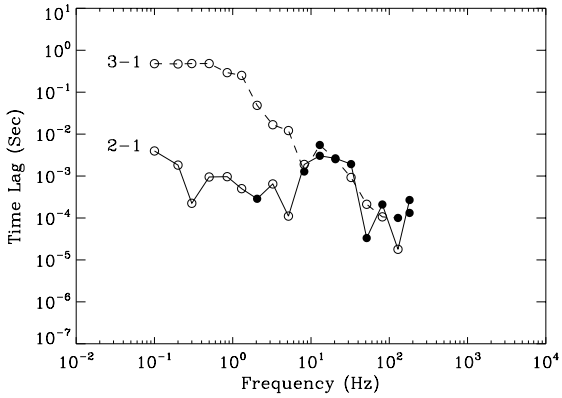

FIG. 10*b*

FIG. 10.—(*a*) Same configuration and parameters as for Fig. 8*a* except for a ring with radii $r_{in} = 4.0$, $r_{out} = 4.5$ lt-s. (*b*) Same as in Fig. 8*b* for the configuration corresponding to (*a*).

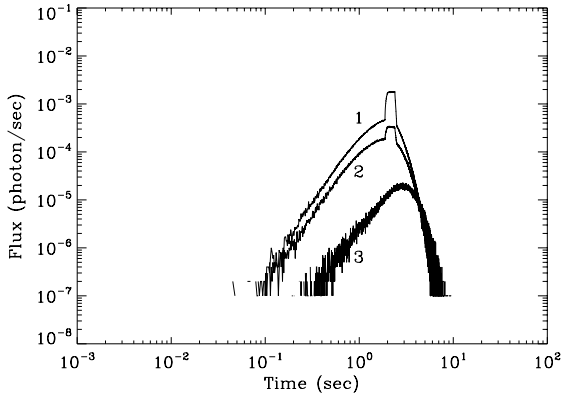

FIG. 11*a*

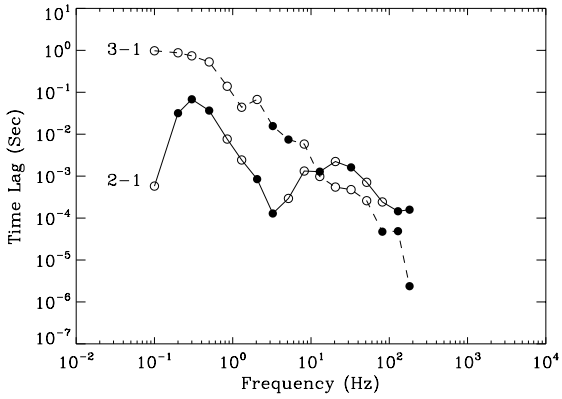

FIG. 11*b*

FIG. 11.—(*a*) Same configuration and parameters as for Fig. 9*a* except for a ring with radii $r_{in} = 4.0$, $r_{out} = 4.5$ lt-s. (*b*) Same as in Fig. 9*b* for the configuration corresponding to (*a*).

the 2–1 curve in Figure 8*b* does exhibit a general trend similar to the linear dependence of the $p = 1$ coronae associated with central photon injection. On the other hand, the form of the 3–1 lag curve is distinctly different from that corresponding to soft photon injection.

Figures 10 and 11 exhibit the effects of the finite size of the soft photon source. In both the $p = 1$ and the $p = 0$ cases, the source's finite extent manifests itself in the light curves as a plateau of duration 0.5 s starting again at $t =$ 2 s, i.e., the light crossing time through the center of the corona. This feature is absent from the light curves of band 3 for the reasons given above. The corresponding lags are now substantially different in shape from those of the corresponding Figures 8*b* and 9*b*, as indicated by the presence of negative lags at progressively low periods (especially in Fig. 10*b*), in qualitative agreement with the arguments made above. These can be understood as the mixing of hard and soft photons due to the finite size of the soft photon source, which becomes more pronounced as the size of the source increases. It is apparent that these lags are very different from those observed in the sources discussed in the previous section, thus making a strong case for the injection of the soft photons at radii considerably smaller than the extent of the Comptonizing coronae.

5. CONCLUSIONS

The main results of the present investigation are the following:

1. Fourier-frequency–dependent, hard X-ray lags appear to be a common property of accreting, Galactic BHCs. Observed first in the hard spectral state of Cyg X-1 (Miyamoto et al. 1988), they appear to be present in its soft state, too (Cui et al. 1997b), and also in a number of other BHC sources. Of particular interest is their apparent increase with period, out to $P \simeq 130$ s in the case of Cyg X-1. Their observed dependence on the Fourier frequency ν has usually the form $\delta t \propto \nu^{-q}$, with q varying between $\simeq 0.6$–1.0.

2. The simplest interpretation of the observed lags is that they are due to the Comptonization process. Then their magnitude provides an estimate of the size of the scattering medium, a quantity inaccessible to spectral modeling. Furthermore, their observed Fourier-frequency dependence can be accounted for by imposing the additional assumption that the Comptonizing plasma is inhomogeneous; the index q of their Fourier-frequency dependence is then found to be related in a simple way to the spatial density profile of the scattering electrons, i.e., the index p (eq. [2]). For $\nu \gtrsim c/r_2$ this relation, as derived from our analytic and numerical calculations, appears to be of the form $q \simeq 2 - p$.

3. Simple analytic models can be used to compute the lags resulting from Comptonization in spherically symmetric, inhomogeneous coronae as a function of the Fourier frequency. We have also used these results to show that these lags, in contrast to the PSD, are generally not affected by variations in the matter accretion rate onto the compact object; as a result they probe properties inherent to the scattering electron cloud rather than to fluctuations in the accretion rate. We have also indicated that our analytic and numerical results, through the relation between the density index p and the lag index q, can be used to *map* the spatial density structure of this class of objects, providing a probe of the dynamics of accreting high-energy sources beyond that afforded by spectral analysis alone. As such, the observed lags associated with BHC sources are in clear disagreement with our models of uniform coronae, while in certain cases they are consistent with the density profiles usually attributed to advection-dominated accretion flows (Narayan & Yi 1994). In most cases they appear consistent with density profiles of the form $n(r) \propto 1/r$, which is not associated with any obvious model of accretion dynamics. The existence of apparently more than one (simple) form for the observed lags raises the possibility of existence of distinct *timing states* for these sources, similar to their well known spectral ones. The (albeit) small number of lag analyses to date indicate that the timing and spectral states are not necessarily correlated, thus raising the possibility of an additional dimension in the study of the issue of the different states of BHC sources.

4. One of the most puzzling and controversial results of the present study is the large sizes of the Comptonizing coronae of BHC sources, implied through our models by the magnitudes of the observed lags; the sizes derived are in excess of 10^{11} cm, several orders of magnitude larger than the horizon size of the putative black holes where most of the accretion energy is thermalized. We do not have, as yet, an obvious mechanism by which the accretion energy can be deposited to energetic electrons over such distances. We consider an account of the observed lags one of the major reasons for vigorously pursuing studies along these lines. On the other hand, it maybe possible for more complicated models to produce the observed lags by processes taking place in a much smaller region, closer to the black hole horizon (e.g., Nowak et al. 1997); however, given the state of these models, we believe that Occam's razor favors, for the time being at least, the ones presented herein.

5. The position and size of the soft photon source have strong effects on the form of the lags as a function of Fourier frequency; the results of our simulations indicate that a soft photon source exterior to the corona produces lags that are, in general, of considerably different form than those due to a source located at its center. The differences become particularly pronounced if the soft photon source is of finite extent, a fact manifested by the presence of negative lags at increasingly larger Fourier periods, and that, as argued in HKT, would greatly reduce their CF. The data from the limited number of sources presented in § 2 seem to favor central rather than exterior soft photon injection.

The results we have presented above were produced under the assumption that the scattering electron cloud is spherically symmetric and optically thin. One expects that at least the first of these assumptions would be violated in realistic sources. However, as long as their overall geometry is not very different from spherical, i.e., the ratio of their largest to their smallest dimensions is not much greater than one, the general conclusions reached above would still hold. If the Thomson depth of these configurations becomes considerably larger than 1, it would first impact the resulting spectra and would also make the parameter α in equation (4) larger, leading to flatter PSDs; such a correlation between the spectral and PSD indices should be searched for in the existing data. Finally, if the source is very asymmetric and sufficiently opaque, both the spectra and the lags should have a strong dependence on the observer's orientation; such a dependence could be uncovered by searching for a correlation of the spectral and timing

properties of these systems with the phase of the binary orbit. We are not at present aware that any such a dependence has been observed in any of the sources discussed above.

In conclusion, timing analysis of BHC sources through the study of time lags appears to be a powerful tool, complementary to the more commonly employed spectral analysis. Both are necessary, however, in order to determine the properties of the Comptonizing coronae of accreting high-energy sources, the latter to provide the temperature and optical depth of the coronae and the former to provide estimates of the physical size (assuming that the lags are due to Comptonization) and spatial distribution of the hot electrons. These results supplemented by further timing analysis through the study of PSDs and moments of the observed light curves are expected to provide additional constraints that will allow the unequivocal determination of the dynamics of accretion onto the compact object.

The authors would like to thank J. C. Ling, J. E. Grove, S. N. Zhang, J. Swank, and W. Focke for useful discussions.

REFERENCES

Belloni, T., et al. 1996, ApJ, 472, L107
Cui, W., et al. 1997a, ApJ, 474, L57
———. 1997b, ApJ, 484, 383
Chen, X., & Taam, R. E. 1995, ApJ, 441, 375
Crary, D. J., et al. 1998, ApJL, 493, L71
Green, A. R., et al. 1993, MNRAS, 265, 664
Grove, J. E., et al. 1997, AIP Conf. Proc. 410, Fourth Compton Symposium, ed. C. D. Dermer (Woodbury, NY: AIP), 122
Grove, J. E., Strickman, M. S., Matz, S., Hua, X.-M., Kazanis, P. R., Titarchuk, L. G. 1998, ApJ, 502, L45
Hua, X.-M. 1997, J. Comput. Phys., 11, 6
Hua, X.-M., Kazanas, D., & Titarchuk, L. 1997, ApJ, 482, L57 (HKT)
Hua, X.-M., & Titarchuk, L. 1995, ApJ, 449, 188
———. 1996, ApJ, 469, 280
Kazanas, D., & Hua, X.-M. 1998, in AIP Conf. Proc. 431, Accretion Processes in Astrophysical Systems, ed. S. S. Holt & T. R. Kallman (New York: AIP), 113
Kazanas, D., Hua, X.-M., & Titarchuk, L. 1997, ApJ, 480, 735 (KHT)
Ling, J. C., et al. 1997, ApJ, 484, 375
Miller, M. C. 1995, ApJ, 441, 770
Miyamoto, S., et al. 1988, Nature, 336, 450
———. 1991, ApJ, 383, 784
Narayan, R., & Yi, I. 1994, ApJ, 428, L13
Nowak, M. A., et al. 1997, ApJ, in press (astro-ph/9810406)
Payne, D. G. 1980, ApJ, 237, 951
Smith, D. M., et al. 1997, ApJ, 489, L51
Sunyaev, R. A., & Titarchuk, L. G. 1980, A&A, 86, 121
Takeuchi, M., Mineshige, S., & Negoro, H. 1995, PASJ, 47, 617
Tennant, A. F., & Mushotzky, R. F. 1983, ApJ, 264, 92
Titarchuk, L. G. 1994, ApJ, 434, 570
van der Klis, M., et al. 1987, ApJ, 319, L13
Vaughan, B. A., & Nowak, M. A. 1997, ApJ, 474, L43
Wijers, R. A. M. J., van Paradijs, J., & Lewin, W. H. G. 1987, MNRAS, 228, 17P
Wilms, J., et al. 1997, AIP Conf. Proc. 410, Fourth Compton Symposium, ed. C. D. Dermer (Woodbury, NY: AIP), 849
Zhang, S. N., Harmon, B. A., Paciesas, W. S., & Fishman, G. J. 1996, IAU Circ. 6405